One radiator with fan has been provided to cool nanofluid after exiting and heating by convection from hot water.

Before starting the experiment tests, water/ethanol solution has been flowing through the system to remove any scales inside the pipes [35]. After filling the cold tank with nanofluid and another hot tank with water, temperature of both water and nanofluid tanks are set, then setting the flow rate of each loop. The system has given enough time to reach steady state of velocity and temperature then recording the temperatures. All experiments have been repeated five times to ensure about repeatability and reproducibility of results.

Nanofluid preparation properties

In order to estimate the nanofluid volume concentrations depending on nanoparticles volume, V_p, and basefluid volume, V_f, respectively eq. (5) below is used:

$$\phi = \frac{V_p}{V_p + V_f} \tag{5}$$

The pH test is using to test the nanofluids stability by OAKTON device for the nanofluid volume fraction. The pH value before and after tests refers to change of thermal properties and the nanofluid stability [23]. Alumina nano solid particle suspended in water as a basefluid undertaken are assumed as a Newtonian fluid, incompressible, single phase flow and an isotropic and all thermophysical properties have been taken form [23] referring to tab. 1.

Table 1. Thermosphysical properties of water and nanoparticles [13]

	Density [kgm^{-3}]	Specific heat capacity [kJkg^{-1}K^{-1}]	Thermal conductivity [Wm^{-1}K^{-1}]
Water	998	4179	0.6
Alumina	3970	765	40

In order to evaluate the nanofluid density, ρ_{nf}, and specific heat capacity, C_{nf}, can be calculated as following equations [16]:

$$\rho_{nf} = \left(\frac{\phi}{100}\right)\rho_p + \left(1 - \frac{\phi}{100}\right)\rho_f \tag{6}$$

$$C_{nf} = \frac{\frac{\phi}{100}(\rho C)_p + \left(1 - \frac{\phi}{100}\right)(\rho C)_f}{\rho_{nf}} \tag{7}$$

The nanoparticles thermal conductivity suspended in the water has been evaluated theoretically by the Maxwell model [16]:

$$k_{nf} = \frac{k_p + 2k_m - 2\varphi(k_w - k_p)}{k_p + 2k_w + \varphi(k_w - k_p)}k_w \tag{8}$$

To estimate the nanofluid viscosity, μ_{nf}, theoretically, Einstein model is adopted as [16]:

$$\mu_{nf} = (1 + 2.5\phi)\mu_f \tag{9}$$

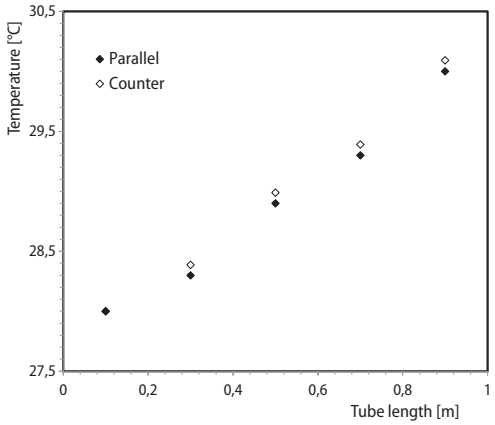

Figure 3. Direction of flow affected to temperature

rection. The temperature profile along the tube length is increasing from inlet to outlet of inner tube by 2 °C for pure water only. The inlet temperatures of inner and outer tubes are 28 °C and 50 °C, respectively.

Figures 4-8 are including six cases that pure water through inner tube, pure water through inner tube is filling porous media, 0.5% nanofluid volume fraction through inner tube, 0.5% nanofluid volume fraction through inner tube is filling porous media, 1% nanofluid volume fraction through inner tube and 1% nanofluid volume fraction through inner tube is filling porous media.

Figure 4 indicates that temperature distribution along tube length under two volume flow-rates 2 Lpm and 5 Lpm. It can be noted that the temperature increases along the tube length for all six cases. The minimum temperature values are found by using pure water in the inner tube, while the maximum temperature values are recorded under using 1% nanofluid and inner tube filling with porous media.

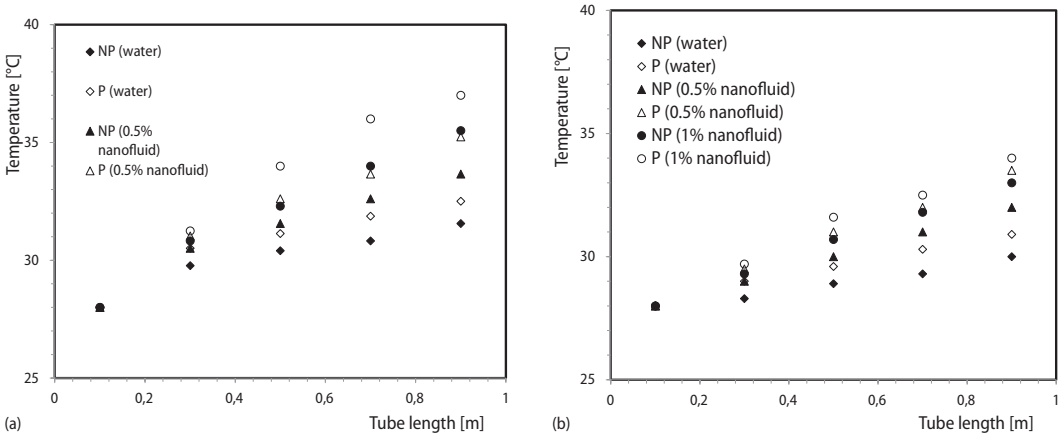

Figure 4. Temperature distribution along tube length for six cases; (a) Q = 2 Lpm and (b) Q = 5 Lpm

Similar behaviors for NTU and effectiveness are shown in figs. 5 and 6. It seems both NTU and effectiveness are increasing as increase in the volume flow-rate and the maximum deviations are 12% and 23%, respectively. Additionally, the using of 1% alumina nanofluid through inner tube filling with porous media has the highest values of NTU and effectiveness. The reason to increase of the NTU and effectiveness values is dependent them on the overall heat transfer coefficient that increasing with increase of nanofluid volume fractions [13].

Figure 7 demonstrates that overall heat transfer coefficient with different volume flow-rates and six cases of this study. It can be seen that the overall heat transfer coefficient increases as increase of volume flow-rates and the deviation between them is approximately 20%. Likewise, it is increased due to increase of porous media size and nanoparticle volume

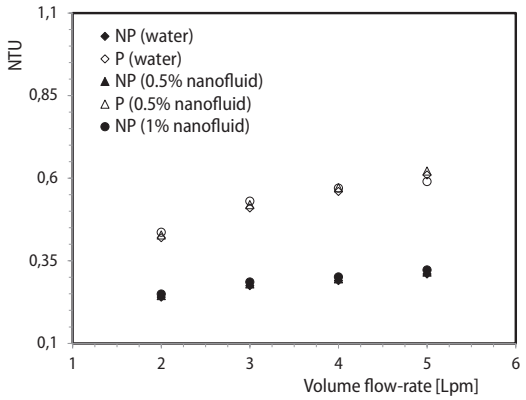

Figure 5. The NTU against volume flow-rate for six cases

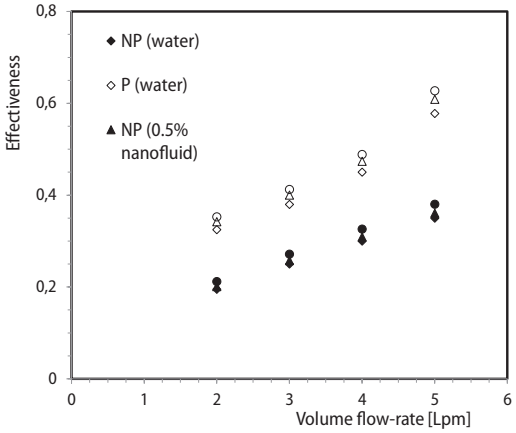

Figure 6. Effectiveness against volume flow-rate for six cases

concentrations. The reason to heat transfer enhancement may be related to the thermal conductivity enhancement of nanofluid and the reduction of boundary-layer on the tube walls by porous media [13].

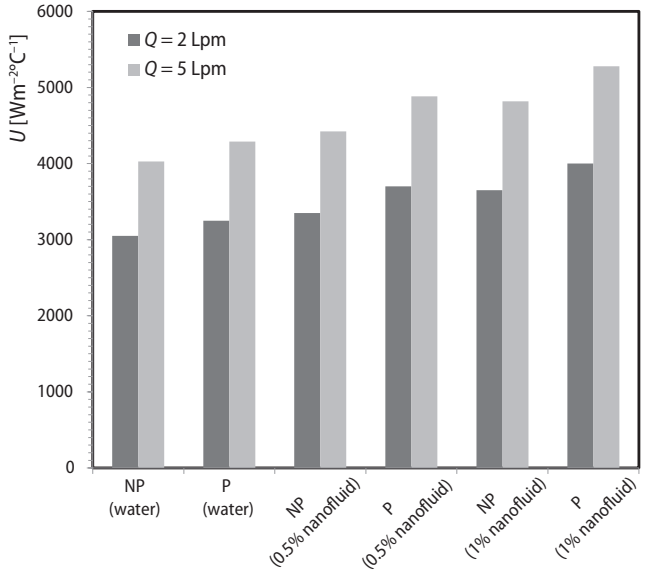

Figure 7. The overall heat transfer coefficient against volume flow-rate for six cases

Conclusions

This project presents an experimental investigation into heat transfer parameter in a double pipe heat exchanger with parallel and counter flow by adding a porous media with size of 3 mm particles and flowing alumina nanofluid with two volume fractions through the inner pipe. While the hot water with constant inlet temperature flow through the outer pipe of the heat exchanger. The experimental tests and theoretical calculations have concluding that:

- The axial temperature profile of outer surface of inner pipe increases towards the ends of heat exchanger with slightly deviation between the counter and parallel flow.

[26] Eagen, J., *et al.,* The Classical Nature of Thermal Conduction in Nanofluids, *ASME J. Heat Transf., 132* (2010), 10, 102402
[27] Lee, J. H., *et al.,* A Review of Thermal Conductivity Data, Mechanics and Models for Nanofluids, *Int. J. Micro-Nano Scale Transp., 1* (2010), 4, pp. 269-322
[28] Fan, J., Wang, L., Review of Heat Conduction in Nanofluids, *ASME J. Heat Transf., 133* (2011), 4, 040801
[29] Nazar, R., *et al.* Mixed Convection Boundary Layer Flow from a Horizontal Circular Cylinder Embedded in a Porous Medium Filled with a Nanofluid, *Transp. Porous Med., 86* (2011), Nov., pp. 517-536
[30] Sheu, L. J., Thermal Instability in a Porous Medium Layer Saturated with a Viscoelastic Nanofluid, *Transp. Porous Media, 88* (2011), Mar., pp. 461-477
[31] Agarwal, S., *et al.,* Non-Linear Convective Transport in a Binary Nanofluid Saturated Porous Layer, *Transp. Porous Med., 93* (2012), 1, pp. 29-49
[32] Hussein, A. M., *et al.,* A Review of Forced Convection Heat Transfer Enhancement and Hydrodynamic Characteristics of a Nanofluid, *Renewable and Sustainable Energy Reviews, 29* (2014), Jan., pp. 734-743
[33] Hussein, A. M., Adaptive Neuro-Fuzzy Inference System of Friction Factor and Heat Transfer Nanofluid Turbulent Flow in a Heated Tube, *Case Studies in Thermal Engineering, 8* (2016), Sept., pp. 94-104
[34] Hussein, A. M., *et al.,* Heat Transfer Enhancement with Elliptical Tube under Turbulent Flow TiO_2-water nanofluid, *Thermal Science, 20* (2016), 1, pp. 89-97
[35] Hussein, A. M., *et al.,* Nanoparticles Suspended in Ethylene Glycol Thermal Properties and Applications: An Overview, *Renewable and Sustainable Energy Reviews, 69* (2017), Mar., pp. 1324-1330

Paper submitted: June 2, 2019
Paper revised: October 12, 2019
Paper accepted: January 29, 2020